JOURNAL OF MATERIALS SCIENCE 35 (2000) 3409–3413

High-temperature thermoelectric properties of the sintered $Bi_2Sr_2Ca_{1-x}Y_xCu_2O_y$ ($x = 0-1$)

M. YASUKAWA*, N. MURAYAMA
National Industrial Research Institute of Nagoya, 1-1 Hirate-cho, Kita-ku, Nagoya 462-8510, Japan
E-mail: murayama@nirin.go.jp

Electrical conductivity and Seebeck coefficient were measured in a temperature range of 320–1073 K for sintered samples of $Bi_2Sr_2Ca_{1-x}Y_xCu_2O_y$ ($x = 0$, 0.2, 0.4, 0.6, 0.8, 1.0). It has been found that the conduction behavior changes from n-type metallic to p-type semiconducting with increasing yttrium concentration. The power factors were in a range of 1.7–3.0 $\times 10^{-5}$ $Wm^{-1} K^{-2}$ for the sample with $x = 0.8$, being maximized by the optimization of the yttrium concentration. The thermal conductivity for the sample with $x = 0.8$ was 0.73 $Wm^{-1} K^{-1}$ at 310 K, and decreased with increasing temperature. The values of thermoelectric figure of merit were estimated to be in a range of 3.4–4.8 $\times 10^{-5}$ K^{-1} at temperatures of 320–673 K for the sample with $x = 0.8$.

1. Introduction

Thermoelectric figure of merit (Z) is defined by an equation: $Z = S^2\sigma\kappa^{-1}$, where S, σ, and κ are Seebeck coefficient, electrical conductivity, and thermal conductivity, respectively. The larger values of $|S|$ and σ and the smaller κ are required for a material with higher Z value. Dimensionless figure of merit (ZT) is a parameter to judge the possibility of thermoelectric application: the satisfaction of $ZT \geqq 1$ is a criterion for the practical use of a material. It has been satisfied for alloys and compounds based on Bi_2Te_3 [1], PbTe [1], SiGe [1], and $CeFe_4Sb_{12}$ [2]. However, the practical use of the materials is limited to the conditions at lower temperatures or under vacuum, because of the relatively low melting points or easiness of oxidation. On the other hand, oxide materials with high ZT values can be used at high temperatures in air for a long time as the thermoelectric energy conversion materials. The possibility of thermoelectric application has been investigated for many oxide materials. It was reported that the perovskite-type compounds such as $La_{0.1}Ba_{0.9}TiO_3$ [3], $La_{0.08}Ca_{0.92}MnO_3$ [3], $(R_{1-x}Ca_x)MnO_3$ (R = Tb, Ho, Y) [4], and $Ba_{1-x}Sr_xPbO_3$ [5, 6] exhibited Z values higher than 10^{-4} K^{-1}. The ZnO-based compounds such as $Zn_{1-x}Al_xO$ [7] and $(ZnO)_mIn_2O_3$ homologous series [8] were also reported to exhibit similar Z values. The layered oxide of $NaCo_2O_4$ [9] and the porous Y_2O_3 [10] have recently been found to be nearly $ZT = 1$.

Mason *et al.* [11–14] investigated the possibility of thermoelectric application for several high-T_c superconducting cuprates (HTSCs) on the basis of the Seebeck coefficient as a function of the electrical conductivity, and reported that the HTSCs could operate as the passive thermoelectric materials because of the small power factors ($S^2\sigma$). However, the investigations of the thermoelectric properties as a function of temperature may give an insight to develop the possibility of thermoelectric application. Moreover, the oxide materials with perovskite-related structures such as HTSCs are objects of searching new thermoelectric materials. One reason is the high capability for doping. It leads to the formation of the solid solutions over the wide composition range and makes possible to control the electrical conductivity from metallic to insulating or between p-type and n-type as well as the thermal conductivity.

$Bi_2Sr_2CaCu_2O_y$ is a layered compound with $n = 2$ of the $Bi_2Sr_2Ca_{n-1}Cu_nO_y$ ($n = 1$, 2, 3) homologous series and is an 80 K superconductor [15]. Substitution of Ca with Y leads to the formation of the $Bi_2Sr_2Ca_{1-x}Y_xCu_2O_y$ solid solutions over the entire composition range of x [15–17]. Temperature dependence of the electrical resistivity at temperatures lower than 300 K shows metallic behavior for the samples with $x \leqq 0.4$ and semiconducting one for those with $x \geqq 0.5$ [15–17]. The superconducting transitions are observed for $x \leqq 0.5$, T_c being maximized at a composition with $x = 0.2$ [17]. Temperature dependence of the Seebeck coefficient for $Bi_2Sr_2CaCu_2O_y$ ($x = 0$) shows n-type metallic behavior in a temperature range of $T_c - 300$ K: the Seebeck coefficient linearly decreases from 0 at T_c to negative values with increasing temperature [18–21]. The Seebeck coefficient increases with increasing x for the $Bi_2Sr_2Ca_{1-x}Y_xCu_2O_y$ system at temperatures lower than 300 K [18–21]. For the samples with $x = 0.1$–0.4, the Seebeck coefficient rapidly increases from 0 to positive values and almost linearly

* *Present Address:* CREST, Japan Science and Technology Corporation (JST), 4-1, Kagamiyama 1 chome, Higashi-Hiroshima 739-8527, Japan.

decreases with increasing temperature [19–21]. For the samples with $x \geqq 0.6$, the Seebeck coefficient gradually increases with increasing temperature [20, 21]. Thus, the $Bi_2Sr_2Ca_{1-x}Y_xCu_2O_y$ system shows conduction behaviors of n-type metal for $x = 0$, p-type metal for $x = 0.1$–0.4, and p-type semiconductor for $x = 0.5$–1.0 at temperatures lower than 300 K, indicating the metal-insulator (M-I) transition at a composition near $x = 0.5$.

Ponnambalam *et al.* [22] investigated the electrical resistivity and the Seebeck coefficient for sintered bodies of $Bi_2Sr_2Ca_{1-x}Y_xCu_2O_y$ with $x = 0.5$–1.0 in a temperature range of 300–700 K. They reported that the materials exhibited p-type semiconducting behavior [22]. The highest Z value was estimated to be $1.9 \times 10^{-5}\,K^{-1}$ for the sample with $x = 0.7$ using the thermal conductivity ($1.2\,Wm^{-1}\,K^{-1}$) in a literature [23]. However, the estimation of figure of merit using σ, S, and κ measured for a material will give more valid value. Moreover, the drastic change in the conduction behavior with increasing x observed at temperatures lower than 300 K motivates us to investigate the thermoelectric properties at elevated temperatures over the whole composition range of x.

In this study, the electrical conductivity and the Seebeck coefficient have been measured in a temperature range of 300–1073 K for sintered bodies of $Bi_2Sr_2Ca_{1-x}Y_xCu_2O_y$ with $x = 0$, 0.2, 0.4, 0.6, 0.8, and 1.0. The figure of merit is estimated from σ, S, and κ measured for the sample with $x = 0.8$.

2. Experimental

Sintered samples of $Bi_2Sr_2Ca_{1-x}Y_xCu_2O_y$ ($x = 0$, 0.2, 0.4, 0.6, 0.8, and 1.0) were prepared from reagent grade Bi_2O_3, $SrCO_3$, $CaCO_3$, Y_2O_3, and CuO powders. The stoichiometric mixture was calcined at 1073 K for 24 h in air with an intermittent grinding. The calcined powder was pelletized and heated at 1123 K for 80 h in air with the intermittent grindings. For densification, the pellet was hot-forged at 1073 K under 2.0 MPa for 2 h in air followed by the hot-forging at 1123 K under 7.4 MPa for 2 h. Powder X-ray diffraction (XRD) patterns were measured with a Philips APD-1700 diffractometer (Cu K_α radiation). The lattice parameters were determined using Si as an internal standard.

Thermoelectric properties were measured by the same way as described in the previous papers [5, 6, 24]. Rectangular sample was cut from the sintered pellet. Two gold wires were tightly bound around the sample. Platinum sheet electrodes, to each of which a platinum wire and a Pt-Pt13%Rh thermocouple were fixed, were mechanically attached to both sides of the sample through gold thin foils in order to avoid the reaction between the sample and the platinum. Electrical conductivity and Seebeck coefficient were measured at several constant temperatures of 320–1073 K in air along the direction perpendicular to the forging direction. The former was measured by d.c. four-probe method. Temperature difference (ΔT) and thermoelectromotive force (ΔV) between the ends of the sample were measured using the thermocouples and the platinum wires, respectively. By controlling the flow rate of the air, which blows one side of the sample through silica tube, ΔT was steadily changed within 10 K. The Seebeck coefficient was calculated from the linear gradient of $\Delta V/\Delta T$, and was corrected for the thermopower of platinum [25].

Thermal diffusivity and specific heat were measured on the disk sample along the forging direction in a temperature range of 310–673 K under vacuum by laser flash method (ULVAC TC-3000). Pulsed ruby laser with width of 800 μs was used as a heat source, so that the finite pulse-width effect could be neglected. An InSb infrared detector was used at 77 K for the thermal diffusivity measurement. The thermal diffusivity was corrected for the heat loss effect using the method of Heckman [26]. The specific heat was measured using a Pt-Pt13%Rh thermocouple (0.1 mm-diameter) fixed on the sample surface. A sapphire was used as a standard of the specific heat. Thermal conductivity was estimated as the product of bulk density at room temperature, thermal diffusivity, and specific heat measured on a sample.

3. Results and discussion

Powder XRD patterns were indexed on the basis of pseudotetragonal unit cell for the samples with $x = 0$, 0.2, 0.4 and orthorhombic one for those with $x = 0.6$, 0.8, 1.0. The changes in the lattice parameters a, b, c with increasing yttrium concentration are shown in Fig. 1. The parameters a and b increased with increasing x whereas the c decreased. The lattice parameters agreed well with those of the literature [17], indicating the formation of the $Bi_2Sr_2Ca_{1-x}Y_xCu_2O_y$ solid solutions. The relative densities of the sintered bodies were estimated to be higher than 85% of the theoretical ones.

Temperature dependence of the electrical conductivity is shown in Fig. 2. The conductivities decreased with increasing yttrium concentration over the measured temperature range. There is a difference by more than 4 orders of magnitude between the conductivities at 320 K for the samples with $x = 0$ and 1. The

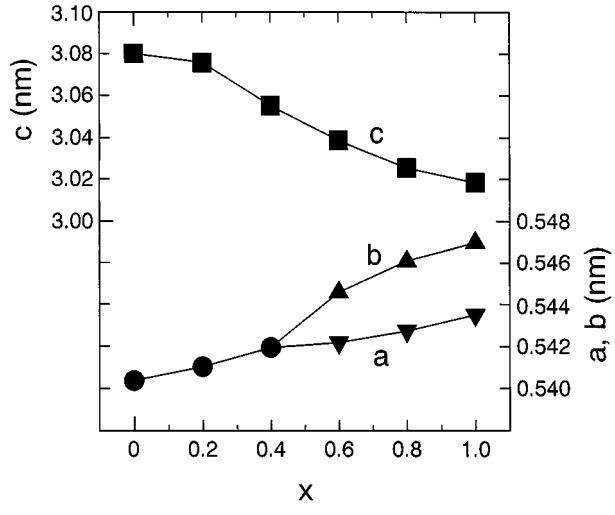

Figure 1 Variations of the lattice parameters a, b, and c with increasing yttrium concentration (x). The powder XRD patterns were indexed with pseudotetragonal unit cell for the samples with $x = 0$, 0.2, and 0.4 whereas those were indexed with orthorhombic one for $x = 0.6$, 0.8, and 1.0.

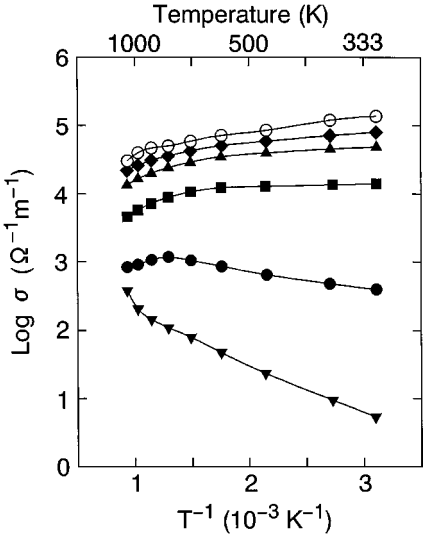

Figure 2 Temperature dependence of the electrical conductivity for sintered samples of $Bi_2Sr_2Ca_{1-x}Y_xCu_2O_y$. Key: (○) $x = 0.0$, (♦) $x = 0.2$, (▲) $x = 0.4$, (■) $x = 0.6$, (●) $x = 0.8$, (▼) $x = 1.0$.

conductivity decreased with increasing temperature for the samples with $x = 0$, 0.2, 0.4, and 0.6 showing the metallic behavior, whereas that increased for the sample with $x = 1$ showing the semiconducting behavior. Temperature dependence of the conductivity for the sample with $x = 0.8$ showed M-I transition at 773 K.

Temperature dependence of the Seebeck coefficient is shown in Fig. 3. The Seebeck coefficient increased with increasing x over the measured temperature range except for the values at temperatures higher than 870 K for the sample with $x = 1$. The signs of the Seebeck coefficient were negative for the samples with $x = 0$ and 0.2 except for the value at 320 K for $x = 0.2$, whereas those were positive for the samples with $x = 0.4$, 0.6, 0.8, and 1.0 except for the value at 1070 K for $x = 1$. For the samples with $x = 0$, 0.2, 0.4, and 0.6, the Seebeck coefficient decreased with increasing temperature at lower temperatures while increased at higher temperatures. Those for the samples with $x = 0.8$ and 1.0 decreased with increasing temperature, although a bend was observed at 770 K for $x = 0.8$, which is consistent with the M-I transition observed on the conductivity data. The data of the Seebeck coefficient measured in this study are well connected to the previous data [20, 21] measured at temperatures lower than room temperature. The Seebeck coefficients at temperatures lower than room temperature also increased with increasing x and showed the sign reversal between the samples with $x = 0$ and 0.1 [20, 21]. The change in the Seebeck coefficient with changing yttrium concentration and temperature was discussed by the two-band model based on the coexistence of electrons and holes [19, 20]. The observed change in the sign of the Seebeck coefficient may support this model. Thus, the conduction behavior in the $Bi_2Sr_2Ca_{1-x}Y_xCu_2O_y$ system changes from n-type metallic to p-type semiconducting with increasing x. The M-I transition seems to occur in a composition range of $0.6 < x < 1.0$.

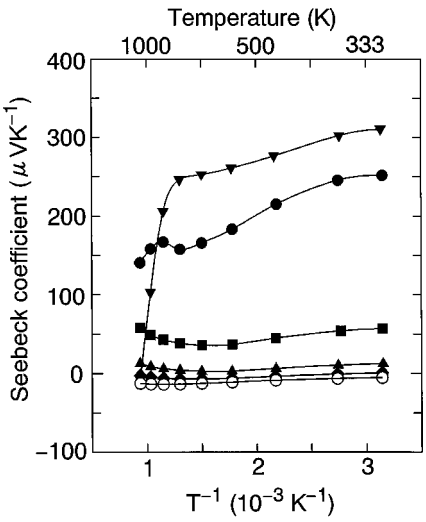

Figure 3 Temperature dependence of the Seebeck coefficient for sintered samples of $Bi_2Sr_2Ca_{1-x}Y_xCu_2O_y$. Key: (○) $x = 0.0$, (♦) $x = 0.2$, (▲) $x = 0.4$, (■) $x = 0.6$, (●) $x = 0.8$, (▼) $x = 1.0$. The thermopower data were corrected for the absolute thermopower of platinum [25].

Temperature dependence of the power factor ($S^2\sigma$) is shown in Fig. 4. The power factors are in a range of 1.3–4.6 $\times 10^{-5}$ $Wm^{-1}K^{-2}$ for the samples with $x = 0.6$ and 0.8, whereas those for the others are less than 10^{-5} $Wm^{-1}K^{-2}$. Since the conductivities decrease with increasing x whereas the Seebeck coefficients increase, the higher power factors for the samples with $x = 0.6$ and 0.8 are due to the optimization of the yttrium concentration. At temperatures higher than 463 K, the power factors for $x = 0.8$ are higher than those for $x = 0.6$ and also a little higher than those (2.0–2.6 $\times 10^{-5}$ $Wm^{-1}K^{-2}$) for $x = 0.7$ reported by Ponnambalam *et al.* [22].

Temperature dependence of the thermal conductivity for the sample with $x = 0.8$ is shown in Fig. 5. The thermal conductivity was 0.73 $Wm^{-1}K^{-1}$ at 310 K and decreased with increasing temperature. The value at 310 K is lower than that (1.2 $Wm^{-1}K^{-1}$) extrapolated to 300 K of the data for Bi-Sr-Ca-Cu-O sample reported by Peacor *et al.* [23]. The thermal conductivity (κ) is expressed by a sum of the lattice part (κ_l) and the electronic one (κ_e): $\kappa = \kappa_l + \kappa_e$. The substitution of Ca with Y will lead to the decrease in the lattice thermal conductivity due to the increase in the phonon scattering

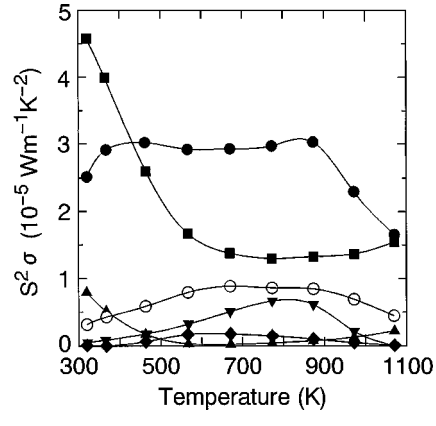

Figure 4 Temperature dependence of the power factor ($S^2\sigma$) for sintered samples of $Bi_2Sr_2Ca_{1-x}Y_xCu_2O_y$. Key: (○) $x = 0.0$, (♦) $x = 0.2$, (▲) $x = 0.4$, (■) $x = 0.6$, (●) $x = 0.8$, (▼) $x = 1.0$.

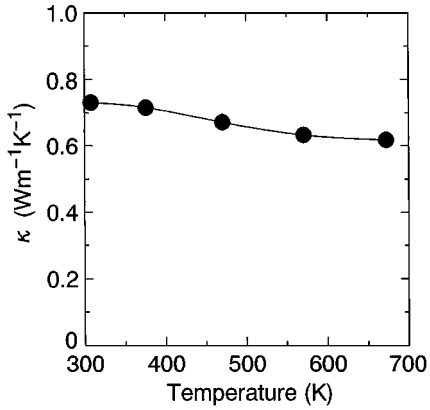

Figure 5 Temperature dependence of the thermal conductivity for the sample with $x = 0.8$.

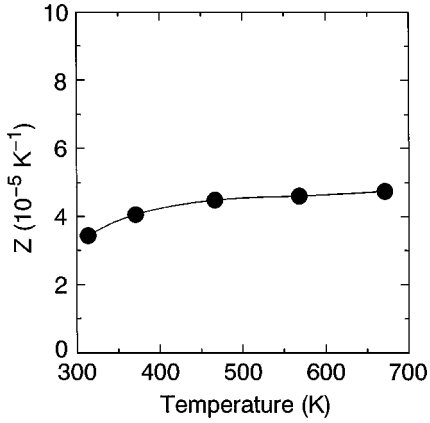

Figure 6 Temperature dependence of the figure of merit (Z) for the sample with $x = 0.8$.

center. The electronic thermal conductivity is related to the electical conductivity by Wiedemann-Franz law: $\kappa_e = L\sigma T$, where L is the Lorenz number. As shown in Fig. 2, the electrical conductivity decreased by more than 2 orders of magnitude with increasing yttrium concentration from $x = 0$ to 0.8. Therefore, the lower thermal conductivity for the sample with $x = 0.8$ compared to the yttrium non-doped sample can be attributed to both the decreases in the lattice and the electronic parts.

Temperature dependence of the figure of merit (Z) for the sample with $x = 0.8$ is shown in Fig. 6. The Z values are in a range of $3.4–4.8 \times 10^{-5}$ K^{-1} and higher than that (1.9×10^{-5} K^{-1}) for the sample with $x = 0.7$ reported by Ponnambalam *et al.* [22]. However, the Z values are lower by about 2 orders of magnitude than those for the Bi_2Te_3-based material [27, 28]. Since the thermal conductivities for the $Bi_2Sr_2Ca_{0.2}Y_{0.8}Cu_2O_y$ sample are lower than those for the Bi_2Te_3-based material [27, 28], the lower Z values for the former can be attributed to the lower power factors, which are in a range of $1.7–3.0 \times 10^{-5}$ Wm^{-1} K^{-2} and comparable to those for the sintered samples of $Nd_{2-x}Ce_xCuO_4$ [29] and the other HTSCs [11]. The power factors are limited to less than 10^{-4} Wm^{-1} K^{-2} at present for the HTSCs in which the trade-off relationship between S and σ is observed as shown in this study. Therefore, the drastic improvement of the power factor is required to find the possibility of thermoelectric application for the $Bi_2Sr_2Ca_{1-x}Y_xCu_2O_y$ system. An approach to be considered is the use of the crystal anisotropy. Single crystalline sample may exhibit a power factor along the direction in the *ab* plane higher than that along the *c*-axis direction due to the higher electrical conductivity, although there may be also the anisotropy in the thermal conductivity and/or the Seebeck coefficient. The investigations of the anisotropy in σ, S, and κ for yttrium-doped single crystals will make this problem clear.

4. Conclusions

Electrical conductivity and Seebeck coefficient were measured in a temperature range of 320–1073 K for sintered samples of $Bi_2Sr_2Ca_{1-x}Y_xCu_2O_y$ ($x = 0$, 0.2, 0.4, 0.6, 0.8, and 1.0). It has been found that the conduction behavior changes from n-type metallic to p-type semiconducting with increasing yttrium concentration. The sign reversal of the Seebeck coefficient occurs at compositions of $x \sim 0.2$. The M-I transition takes place in a composition range of $0.6 < x < 1.0$. The power factors for the sample with $x = 0.8$ were in a range of $1.7–3.0 \times 10^{-5}$ Wm^{-1} K^{-2}, being maximized by the optimization of the yttrium concentration. The thermal conductivity for $x = 0.8$ was 0.73 Wm^{-1} K^{-1} at 310 K and decreased with increasing temperature. The values of figure of merit were estimated to be in a range of $3.4–4.8 \times 10^{-5}$ K^{-1} at temperatures of 320–673 K for $x = 0.8$.

References

1. D. M. ROWE, in "CRC Handbook of Thermoelectricity," edited by D. M. Rowe (CRC Press, Boca Raton, 1995) p. 441.
2. B. C. SALES, D. MANDRUS and R. K. WILLIAMS, *Science* **272** (1996) 1325.
3. F. S. GALASSO, in "Structures, Properties, and Preparation of Perovskite-type Compounds" (Pergamon Press, Oxford, 1969) p. 73.
4. T. KOBAYASHI, H. TAKIZAWA, T. ENDO, T. SATO, M. SHIMADA, H. TAGUCHI and M. NAGAO, *J. Solid State Chem.* **92** (1991) 116.
5. M. YASUKAWA and N. MURAYAMA, *J. Mater. Sci. Lett.* **16** (1997) 1731.
6. *Idem., Mater. Sci. Eng.* **B54** (1998) 64.
7. M. OHTAKI, T. TSUBOTA, K. EGUCHI and H. ARAI, *J. Appl. Phys.* **79** (1996) 1816.
8. M. KAZEOKA, H. HIRAMATSU, W.-S. SEO and K. KOUMOTO, *J. Mater. Res.* **13** (1998) 523.
9. H. YAKABE, K. KIKUCHI, I. TERASAKI, Y. SASAGO and K. UCHINOKURA, in Proceedings of the 16th International Conference on Thermoelectrics, Dresden, Germany, 1997, p. 523.
10. K. KOUMOTO, W.-S. SEO and S. OZAWA, *Appl. Phys. Lett.* **71** (1997) 1475.
11. T. O. MASON, *Mater. Sci. Eng.* **B10** (1991) 257.
12. M.-Y. SU, C. E. ELSBERND and T. O. MASON, *Physica C* **160** (1989) 114.
13. *Idem., J. Amer. Ceram. Soc.* **73** (1990) 415.
14. M.-Y. SU, E. A. COOPER, C. E. ELSBERND and T. O. MASON, *ibid.* **73** (1990) 3453.
15. A. MAEDA, M. HASE, I. TSUKADA, K. NODA, S. TAKEBAYASHI and K. UCHINOKURA, *Phys. Rev.* **B41** (1990) 6418.
16. R. YOSHIZAKI, Y. SAITO, Y. ABE and H. IKEDA, *Physica C* **152** (1988) 408.
17. T. TAMEGAI, K. KOGA, K. SUZUKI, M. ICHIHARA, F. SAKAI and Y. IYE, *Jpn. J. Appl. Phys.* **28** (1989) L112.

18. C. N. R. RAO, T. V. RAMAKRISHNAN and N. KUMAR, *Physica C* **165** (1990) 183.
19. F. MUNAKATA, K. MATSUURA, K. KUBO, T. KAWANO and H. YAMAUCHI, *Phys. Rev.* **B45** (1992) 10604.
20. J. B. MANDAL, S. KESHRI, P. MANDAL, A. PODDAR, A. N. DAS and B. GHOSH, *ibid.* **B46** (1992) 11840.
21. J. B. MANDAL, A. N. DAS and B. GHOSH, *J. Phys. Condens. Matter.* **8** (1996) 3047.
22. V. PONNAMBALAM and U. V. VARADARAJU, *Physica C* **227** (1994) 102.
23. S. D. PEACOR and C. UHER, *Phys. Rev.* **B39** (1989) 11559.
24. M. YASUKAWA and N. MURAYAMA, *Physica C* **297** (1998) 326.
25. N. CUSACK and P. KENDALL, *Proc. Phys. Soc. London* **72** (1958) 898.
26. R. C. HECKMAN, *J. Appl. Phys.* **44** (1973) 1455.
27. W. M. YIM, E. V. FITZKE and F. D. ROSI, *J. Mater. Sci.* **1** (1966) 52.
28. W. M. YIM and F. D. ROSI, *Solid State Electr.* **15** (1972) 1121.
29. M. YASUKAWA and N. MURAYAMA, *J. Mater. Sci.* **32** (1997) 6489.

Received 25 February
and accepted 16 December 1999